Macromolecules

ARTICLE

pubs.acs.org/Macromolecules

Glass Transition Temperature of Polymer Nanoparticles under Soft and Hard Confinement

Chuan Zhang, Yunlong Guo, and Rodney D. Priestley*

Department of Chemical and Biological Engineering, Princeton University, Princeton, New Jersey 08544, United States

ABSTRACT: When confined to the nanoscale, the glass transition temperature (T_g) of polymer films can deviate substantially from the bulk, i.e., the T_g-confinement effect. Due to ease of processing most studies have focused on the thickness-dependent T_g of thin films, while few have focused on extending investigations beyond thin films to other geometries. As polymers confined to higher geometrical dimensionalities become the enabling material in technologies ranging from drug delivery to plastic electronics to ultrafiltration, a greater understanding of size effects on the T_g is warranted. Here, we investigate the effects of three-dimensional confinement on the T_g of polymer nanoparticles under soft and hard confinement and quantitatively compare our results to those of thin films to explore commonalities or differences between the T_g-confinement effect for polymers confined to different geometries. Via modulated differential scanning calorimetry, we show that T_g decreases with size for polystyrene (PS) nanoparticles suspended in an aqueous solution, in agreement with the corresponding freestanding films. Furthermore, capping of PS nanoparticles with a hard silica shell leads to a size invariant T_g. These results suggest that the free surface is a key factor in T_g reductions of confined polymer, irrespective of geometry.

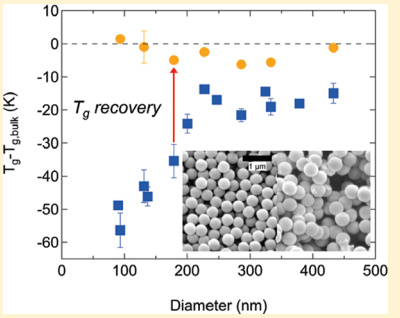

INTRODUCTION

The properties of polymers confined to the nanoscale are of considerable scientific and technological interest. Nanoconfined polymer constitutes the matrix of polymer nanocomposites, and it is their deviation in properties from the bulk that can result in the significant enhancement in the properties of such composites.[1−4] Understanding the properties of polymers confined to the nanometer length scale is key in a wide array of fields from organic electronics[5] to polymeric membranes[6] to drug delivery via polymeric carriers.[7]

The deviation of the glass transition temperature (T_g) from the bulk with decreasing size to the nano length scale, i.e., T_g-confinement effect, has been predominately investigated for thin polymer films, the case of one-dimensional confinement. The discoveries that polystyrene (PS) films supported on silica exhibited a reduction in T_g with decreasing thickness,[8] whereas poly(methyl methacrylate) (PMMA) films exhibited a thickness-dependent T_g that was impacted by the type of supporting substrate,[9] i.e., an increase in T_g with decreasing size for PMMA on silicon and a decrease in T_g with decreasing size for PMMA on gold, has led to a vast scientific endeavor spanning greater than a decade and a half to not only corroborate and understand the effects but also explore the generality of the phenomenon. For example, dielectric relaxation spectroscopy (DRS),[10,11] fluorescence spectroscopy,[12] and viscosity measurements,[13] as well as computational studies,[14] have all revealed a similar reduction in T_g for supported PS thin films on silica. Furthermore, many studies have extended the focus from the T_g-confinement effect in singly supported polymer thin films toward that of doubly supported films,[15] freestanding films,[16,17] and even to polymer nanocomposites[15,18,19] where the polymer, i.e., the matrix, is nanoscopically confined between neighboring inorganic nanoparticles. In addition to exploring the glass transition dynamics, other important properties, such as the creep compliance[20] and physical aging,[21] have been previously examined in nanoconfined polymer thin films. While the present work is focused on polymeric glass-formers, we note that confinement effects have been observed in organic molecular glass-formers, as reported in the seminal study in which *o*-terphenyl exhibited a reduced T_g when confined into controlled pore glass,[22] as well as in other studies that probed the molecular dynamics of organic molecular glass-formers in nanopores.[23−25]

When discussing nanoscopically confined polymer, two effects are generally highlighted: (i) size effects and (ii) interfacial effects. Size effects are purported to occur when the length scale of the confining dimension, i.e., thickness in thin films, and the length scale governing T_g, i.e., a cooperatively rearranging region, coincide.[10,26] Interfacial effects are expected to increase in significance with an increase in the ratio of interfacial surface area to volume.[8,9,12,16] It is the interplay between size and interfacial effects that result in a wealth of interesting observations including substantial increases[9,15] or decreases[8,16,27] in T_g. Factors that influence the deviation in T_g with confinement include geometry,[15,16,28] strength of interfacial interactions,[29] sample preparation and measurement environment,[30] and chemical structure.[27,31]

Received: November 28, 2010
Revised: April 6, 2011
Published: April 19, 2011

There has been growing evidence that the T_g-confinement effect is intimately related to the presence of interfacial effects perturbing glass transition dynamics.[10,12−17,21,31−34] In the case of supported films, interfacial effects occur from the free surface or polymer−substrate interface, with the conventional view being that free surfaces act to locally enhance segmental dynamics leading to a T_g decrease while the attractive interactions between the polymer and substrate act to locally reduce segmental dynamics leading to a T_g increase.[10,12−15,21,31−35] The importance of interfaces in modifying the T_g of polymer films has been highlighted by the observation of freestanding polymer films of PS exhibiting an even greater T_g reduction with confinement than supported PS films,[16,17] the ability to suppress the T_g-confinement effect of supported PS films by capping the free surface,[32] and the finding that doubly silica-supported PMMA films exhibit a greater T_g increase with confinement than singly supported films.[15] Spatially resolved measurements of the local near free surface T_g of PS[12,33] and PMMA[31,34,35] or near substrate T_g of PMMA[31,35] reported lower and higher interfacial T_gs, respectively, a trend in agreement with the size dependence of T_g of the corresponding supported or freestanding polymer films.

However, it must be stated that the impact of confinement on T_g (and the origins of its effect) are still very much a subject matter of debate.[36] An example of the ongoing debate is found in the T_g of supported ultrathin PS films, where depending on the rate of cooling during the measurement of T_g different groups have concluded that the T_g of PS films was reduced with confinement,[8,12,13,37,38] while others argue no change in T_g with confinement.[39,40] A recent study has provided a viable resolution to the contradictory observations, i.e., that the deviation from bulk T_g of ultrathin PS films was strongly dependent on cooling rate.[38] Yet, there are still studies that observe no change in T_g with confinement of thin polymer films where no resolution to opposing views currently exist.[41,42]

Whereas many studies have focused on the size-dependent T_g of thin films, nanotechnology demands the use of confined polymer of different geometries from nanoparticles to nanocomposites to polymer filled nanospheres and cylinders. For example, polymeric nanoparticles with sub-100 nm diameters can serve as the delivery vehicle for pharmaceuticals,[7] and core−shell polymer/inorganic nanoparticles are used as fillers in thin films to operate as photonic and plasmonic structures.[43] While there has been interest in determining the generality of the T_g-confinement effect, only a handful of studies have focused on extending investigations beyond the thin film geometry, i.e., polymer nanoparticles,[28,44,45] polymers confined in nanopores,[46−50] polymer nanocomposites,[15,18,19] and polymer/layered silicate nanostructures.[51−54] This study, which uses modulated differential scanning calorimetry (MDSC) to measure the T_g of suspended polymer nanoparticles and polymer/silica core−shell nanoparticles, is the first to investigate the size dependence of T_g for 3-dimensionally confined polymer under soft (aqueous suspended PS particles) and hard (PS/silica core−shell particles) confinement and reveals the importance of interfacial effects in modifying T_g of confined polymer irrespective of geometry.

EXPERIMENTAL SECTION

Materials Synthesis. PS nanoparticles were synthesized from surfactant-free emulsion polymerization in accordance with procedures described in details elsewhere.[55] Desired nanoparticle sizes were achieved by changing the styrene monomer concentration, initiator concentration, and/or initiator type (ammonium persulfate or potassium persulfate). After synthesis, the nanoparticles were washed twice with water through centrifugation and ultimately suspended in water. Hybrid polymer/silica core−shell nanoparticles were prepared by coating a ∼30 nm thick silica shell around PS nanoparticles using a procedure adapted from the Stöber method, as described in details in ref 55. Bulk polymer samples were created for each PS nanoparticle sample by drying the nanoparticles under vacuum and subsequently annealing at 423 K for 20 h.

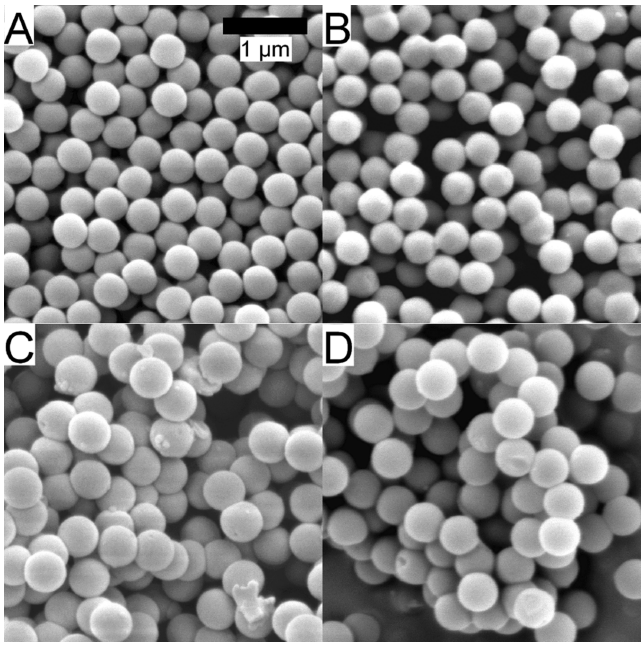

Figure 1. 400 nm diameter PS nanoparticles before (A) and after (B) the measurement of T_g. The corresponding 400 nm diameter PS/silica core−shell nanoparticles (with additional shell thickness of ∼30 nm) before (C) and after (D) the measurement of T_g.

Characterization. Sizes of PS nanoparticles suspended in H_2O were determined from dynamic light scattering (DLS) (Malvern Instruments Zetasizer Nano-ZS ZEN 3600). Weight-average molecular weight (M_w) of each nanoparticle sample in tetrahydrofuran was determined from gel permeation chromatography (GPC) (Waters 515 HPLC pump, Eppendorf CH-460 column heaters, Waters 410 differential refractometer). Images of PS nanoparticles were obtained using scanning electron microscopy (SEM) (FEI XL-30). Nanoparticles were drop-casted onto carbon tape, allowed to dry, and then coated with a 5 nm thick iridium layer prior to imaging. The T_gs of PS nanoparticles suspended in water (and dried PS/silica core−shell nanoparticles) were determined using MDSC (TA Instruments Q2000, second heat with a modulation rate of ±0.200 K/20 s, heating rate of 5 K/min) in hermetically sealed aluminum pans. All reported T_gs are the midpoint value between the tangents of the glass and liquid line from the total heat flow.

RESULTS AND DISCUSSION

In order to provide a meaningful comparison of nanoscale confinement effects on the T_g of polymer nanoparticles suspended in aqueous solution to those of freestanding films, it must first be shown that polymer nanoparticles do not coalesce during the measurement of T_g. Figure 1 shows SEM images of 400 nm diameter PS nanoparticles and the corresponding 400 nm

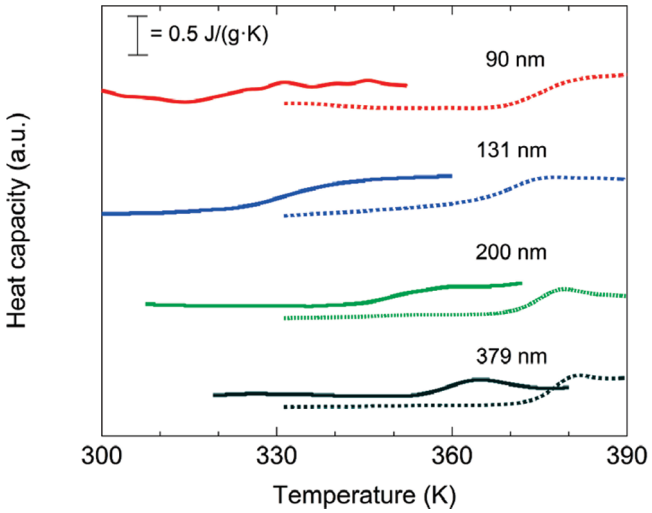

Figure 2. Calorimetric thermograms of several representative PS nanoparticles (solid lines) along with thermograms of the corresponding bulk polymer formed from nanoparticles through thermal annealing (dashed lines).

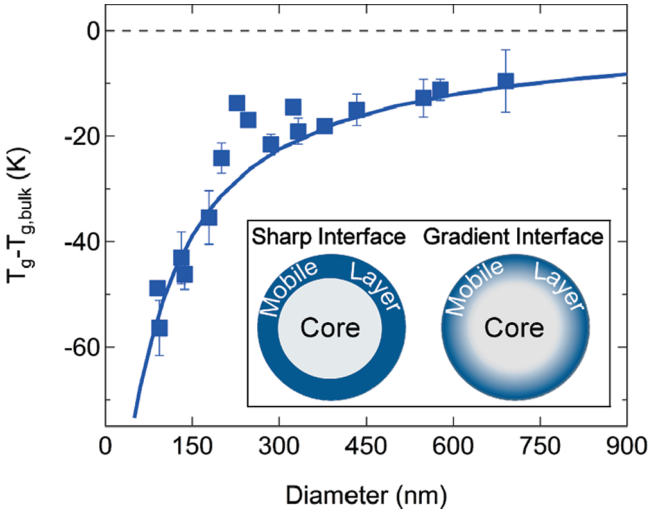

Figure 3. Change in T_g with respect to particle diameter for PS (■) nanoparticles. The solid line is a fit to the PS data using eqs 1−3. Inset schematically compares a sharp vs gradient interface for a layered model.

diameter PS/silica core−shell nanoparticles (with additional shell thickness of ∼30 nm) before and after MDSC. As shown from the representative SEM images, smooth, monodisperse PS nanoparticles could be prepared, and coating of PS nanoparticles with a thin silica shell via a modified Stöber method did not alter the smoothness or monodispersity of the nanoparticles. Most importantly, the images showed that the nanoparticles were neither destroyed nor aggregated during the thermal protocol employed to measure T_g.

Figure 2 shows representative MDSC thermograms of suspended PS nanoparticles ranging from 90 to 379 nm. For each nanoparticle sample, $T_{g,bulk}$ (dashed lines in Figure 2) was measured from nanoparticle samples that were dried under vacuum and subsequently annealed at 423 K for 20 h, which caused the particles to aggregate and form a bulk sample. SEM images (not shown) revealed the formation of bulk polymer by the above annealing protocol. As evident from the thermograms, the T_g of the PS nanoparticles decreased as the size was decreased from 379 to 90 nm, and thus the magnitude of $T_g - T_{g,bulk}$ increased with decreasing size, providing evidence for a larger deviation from the bulk T_g as the PS nanoparticles were further confined.

Figure 3 shows the diameter dependence of $T_g - T_{g,bulk}$ for PS nanoparticles suspended in aqueous solution, i.e., the case of soft confinement. Decreasing the diameter of PS nanoparticles led to a reduced T_g with respect to $T_{g,bulk}$. For PS nanoparticles, the onset diameter for T_g reductions was ∼700 nm. Furthermore, the magnitude of the deviation in T_g with decreasing diameter was significant; e.g., for PS nanoparticles with a diameter of ∼90 nm, $T_g - T_{g,bulk} = -58$ K.

The trend observed in Figure 3 agrees qualitatively with the thickness dependence of T_g for freestanding films of PS.[17] For polymers that show decreases in T_g with confinement, it is now reasonably well accepted that the effect originates at the polymer free surface.[8−10,12−17,31−34] The thickness dependence of T_g is often described via two-layer models.[10,56] The models assume the presence of a mobile layer with enhanced dynamics (or lower T_g) atop a bulk layer with bulk dynamics (or bulk T_g). Although layer models provide successful fits to experimental data, there is growing experimental[12,31,35] and computational[57−59] evidence that suggest T_g perturbations originating at the free surface lead to a distribution of T_gs away from the interface. In formulating a model to describe the diameter dependence of T_g for polymer nanoparticles, we assume (1) the effect originated from a reduction in T_g at the free surface, which in this case is the polymer/water interface, and (2) T_g reductions at the free surface propagated tens of nanometers into the nanoparticle interior. To describe the propagation of surface effects as a function of displacement into the interior of a nanoparticle, an enhanced mobility distribution function ($\xi(r)$) was defined based on the Kohlrausch−Williams−Watts (KWW) equation:

$$\xi(r) = \xi_R \exp[-(R-r)/\lambda]^{\beta} \quad (1)$$

where ξ_R was the magnitude of enhanced surface mobility relative to the bulk (e.g., a ξ_R value of 2 would indicate that the surface mobility is enhanced compared to the bulk mobility by a factor of 2), $R - r$ was the radial distance from the nanoparticle surface, i.e., R was the radius of the nanoparticle and r was a variable denoting the distance from the center of the sphere, λ was the characteristic length (nm), and β was the stretching factor that described the breadth of the distribution. Thus, $\xi(r)$ indicated the increase in mobility relative to the bulk at a distance r from the spherical center. Assuming a spherical nanoparticle, the total volume (V) of the nanoparticle would be given as $V = \int\int\int r^2 \sin\varphi \, dr \, d\varphi \, d\theta$, where φ and θ are the angles of the integral unit. Therefore, a dynamic shell volume (V_d), i.e., the volume that encompasses the region of enhanced mobility, would be defined as

$$V_d = \iiint \xi(r) r^2 \sin\varphi dr d\varphi d\theta \quad (2)$$

The dynamic shell volume can be visualized as a shell layer of enhanced dynamics surrounding the core of the nanoparticle with bulk dynamics. However, we modeled the interface between the two layers of different mobility as a gradient rather than a sharp interface. Figure 3 inset schematically shows the difference of the layer model for a spherical nanoparticle with a sharp and a

dx.doi.org/10.1021/ma1026862 |*Macromolecules* 2011, 44, 4001–4006

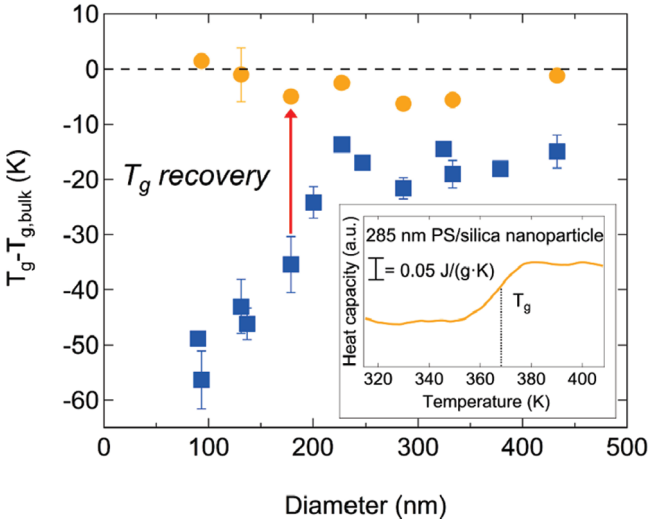

Figure 4. Change in T_g with respect to particle diameter for PS (■) and PS/silica core−shell nanoparticles (●). Inset shows a MDSC thermogram for 285 nm PS/silica core−shell nanoparticles.

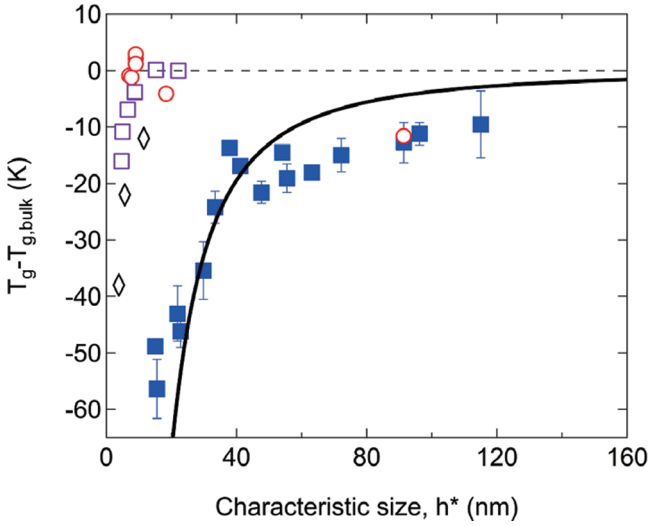

Figure 5. Change in T_g with respect to characteristic size for PS nanoparticles (■) and literature data for PS nanoparticles (○),[28] PS nanoparticles in nanoblend (□),[44] PS domains in block copolymer (◊),[45] and freestanding PS films (solid line).[17]

gradient interface. Assuming the T_g reduction is proportional to the ratio of V_d to V, the diameter dependence of T_g for suspended polymer nanoparticles could then be described by the following equation:

$$T_{g,nanoparticle} = T_{g,bulk} - (T_{g,bulk} - T_{g,surf})V_d/V \qquad (3)$$

where $T_{g,bulk}$ was the bulk T_g of the polymer and $T_{g,surf}$ was the surface T_g of the polymer. The line in Figure 3 is a fit to the data using eqs 1−3 with the fit parameters for PS being ξ_R = 1.91, λ = 9.17 nm, and β = 0.86. $T_{g,surf}$ was taken to be 305 K for PS.[33] The model provided a good fit to the experimental data. As determined from the optimal fit of the model, the distance to which free surface effects penetrated into the nanoparticle core was 33 nm for PS nanoparticles; i.e., at 33 nm, the enhanced mobility distribution, $\xi(r)$, decayed to 95% of the initial value (ξ_R). Earlier NMR studies on 100 nm atactic PS emulsions showed that the polymer surface exhibited a well-defined mobile layer, in which the thickness of the layer was hypothesized to vary as a function of temperature.[60,61] As the temperature approached the bulk T_g, it was determined that the thickness of this mobile layer grew continuously to about 30 nm. From a multilayer/fluorescence study, it was determined that PS films exhibited a distribution of T_gs within the first ∼32 nm of the free surface.[12]

We further explored the free surface as the cause of the reduced T_g for nanoconfined polymer by comparing the size dependence of T_g for suspended PS nanoparticles and the corresponding PS/silica core−shell nanoparticles. Capping of the PS nanoparticles with a silica shell should remove the free surface by confining the polymer within a hard shell, i.e., the case of hard confinement. The thickness dependence of T_g for PS and PS/silica core−shell nanoparticles is shown in Figure 4, with the inset showing a representative MDSC thermogram for a PS/silica core−shell nanoparticle sample. We observed that PS nanoparticles confined within a silica shell did not exhibit a size dependent T_g as observed for bare PS nanoparticles. The T_g recovery can be significant for smaller size nanoparticles, e.g., $T_{g,PS} - T_{g,PS/silica}$ = −42 K for nanoparticles with a diameter of 130 nm. The absence of the T_g-confinement effect for PS/silica core−shell nanoparticles can be partially understood if the free surface is considered a major reason for the size dependence of T_g for polymer nanoparticles. Then it follows that if the silica shell was effective in eliminating the polymer free surface, the T_g-confinement effect, which is a consequence of surface effects, was eliminated. We note that the key observation from Figure 4, i.e., the elimination of the T_g-confinement effect of PS by the removal of the polymer/water interface, is qualitatively consistent with an earlier study performed on PS thin films in which the thickness dependence of T_g for supported PS thin films was eliminated by coating the films with a gold layer atop the free surface.[32]

Capping of PS nanoparticles with a thin silica shell, via the Stöber method, was accomplished at ∼296 K (room temperature). Therefore, at room temperature the nanoparticles should be considered in a stress-free state, and the pressure within the core−shell nanoparticles should be atmospheric. Because of the difference in thermal expansion coefficients between PS and silica, upon heating a positive pressure should develop inside the core−shell nanoparticles. As the T_g of all PS−silica core−shell nanoparticles was near 376 K, i.e., $T_{g,bulk}$, the pressure generated inside the core−shell nanoparticles at T_g would equal ∼60 MPa. For bulk PS, a 60 MPa increase in pressure would increase T_g by ∼15 K.[62] Since the pressure generated during heating can be shown to be independent of nanoparticle size, any T_g enhancement due to pressure would be constant for all core−shell nanoparticles. As such, the complete recovery of $T_{g,bulk}$ for all core−shell nanoparticles, of which the corresponding aqueous suspended nanoparticles showed a greater than 15 K suppression in T_g with confinement (diameter <200 nm), cannot be explained by only pressure effects. For example, $T_g - T_{g,bulk}$ = −58 K and $T_g - T_{g,bulk}$ ∼ 0 K for aqueous suspended PS nanoparticles and PS−silica core−shell nanoparticles, respectively, with a diameter of ∼90 nm. While pressure effects could account for an ∼15 K recovery in the T_g of 90 nm core−shell nanoparticles, the complete recovery can only be explained by considering the impact of the interface on the T_g.

A quantitative comparison of confinement effects on T_g of polymer nanoparticles and freestanding films can be made by defining a characteristic length, h^*, which for nanoparticles was

dx.doi.org/10.1021/ma1026862 |*Macromolecules* 2011, 44, 4001–4006

the volume to surface area ratio and equal to 1/6 of the diameter, whereas for films was taken to be the thickness. According to Figure 5, the size dependence of T_g for PS nanoparticles (■) and PS freestanding films (solid line, fit to PS freestanding films data [M_w = 120−378 kg/mol] taken from ref 17) are in good agreement, despite the fact that the T_gs of films were measured in an air environment, while the T_gs of nanoparticles were measured in an aqueous environment. We note that the M_w range of PS nanoparticles employed in the current study was within the range of 120−378 kg/mol. The consistency in size-dependent T_g of thin films and nanoparticles, when presented as a function of h^*, highlights the importance of the free surface in the T_g-confinement effect.

Figure 5 also plots size-dependent T_g data of PS nanospheres blended into a poly(butyl methacrylate) matrix (□),[44] PS spherical domains within a poly(styrene-*co*-butadiene) matrix (◇),[45] and the only other report (to the best of our knowledge) of PS nanoparticles suspended in an aqueous solution (○).[28] For PS nanospheres embedded into a soft polymer matrix, the onset characteristic size for a thickness-dependent T_g is significantly smaller than that found in the current study for PS nanoparticles and from the literature for PS freestanding films.[17] Nevertheless, beyond the critical onset h^*, embedded PS nanospheres do show a size-dependent T_g. Differences in critical onset h^* may be explained by the presence of the soft matrix interface for embedded PS nanospheres that locally increase the requirement for cooperativity of dynamics in comparison to that of an aqueous or free interface as experienced for PS nanoparticles and freestanding films, respectively. For PS spherical domains within a poly(styrene-*co*-butadiene) matrix, a significant decrease in T_g was observed as the spherical domains decreased in size in the block copolymer, i.e., $T_g - T_{g,bulk} = -38$ K for 23 nm PS spherical domains. However, the authors did not attribute the decrease to an intrinsic size effect, i.e., confinement effect, but rather as a consequence of diffusive interfaces with some degree of intermixing between the phases.[45] This hypothesis was further supported by the lack of a significant T_g deviation for 27 nm PS spherical domains in a styrene−isobutylene−styrene triblock copolymer, where a large difference in the solubility parameters exist between the phases.

In an earlier study on PS nanoparticles suspended in an aqueous environment, no size-dependent T_g was observed, but instead a decrease in the ΔC_p across the glass transition with confinement.[28] The observed decrease in the ΔC_p across the glass transition with confinement was consistent with the results from a 1980 study by Gaur and Wunderlich on dried PS nanoparticles.[63] However, Gaur and Wunderlich did observe a significant broadening in the T_g for the smallest spheres; i.e., the T_g became detectable at approximately $T_{g,bulk} - 40$ K for a 85 nm PS nanoparticle sample on first heating. As discussed in ref 28, the size-invariant T_g of suspended PS nanoparticles could be partially due to a large polydispersity in the molecular weights of the samples, as compared to the nearly monodisperse polymer thin films. Additionally, the presence of a surfactant could have played a role in the size invariance of T_g with decreasing nanoparticle size, although the authors in ref 28 did not observe a T_g deviation as a function of surfactant concentration in the nanoparticle samples. In the current study, PS nanoparticles were prepared by surfactant-free emulsion polymerization, in which all samples exhibited an M_w/M_n ratio of ∼3. Nevertheless, the size-dependent ΔC_p was attributed to the presence of a shell layer with enhanced dynamics surrounding the core with bulk dynamics, a picture consistent with the view taken to describe the current work, previous NMR studies on PS nanoparticles, and freestanding film data.

■ CONCLUSION

In summary, we investigated the size dependence of T_g for PS nanoparticles under soft and hard confinement. We found a striking similarity of size-dependent effects on the T_g for polymer nanoparticles and freestanding films including the magnitude of T_g suppression at a particular characteristic size as well as the ability to suppress the T_g-confinement effect by the capping of the nanoparticle free surface with a hard layer. The observed size dependence of T_g for confined polymer irrespective of geometry suggests a common origin of the T_g-confinement effect. Furthermore, polymer nanoparticles represent a unique system to explore the T_g-confinement effect. Studies investigating the effects of chemical structure, M_w, surfactant type and content, percent cross-linking, and different dispersing media (e.g., glycerol and ionic liquids) are currently underway.

■ AUTHOR INFORMATION

Corresponding Author
*E-mail: rpriestl@princeton.edu.

■ ACKNOWLEDGMENT

We acknowledge usage of the PRISM Imaging and Analysis Center, which is supported in part by the NSF MRSEC program through the Princeton Center for Complex Materials (DMR-0819860). R.D.P. acknowledges the donors of the American Chemical Society Petroleum Research Fund (PRF 49903-DNI10) and the 3M-nontenured faculty grant program for partial support of this work.

■ REFERENCES

(1) Baur, J.; Silverman, E. *MRS Bull.* **2007**, *32*, 328–334.
(2) Paul, D. R.; Robeson, L. M. *Polymer* **2008**, *49*, 3187–3204.
(3) Crosby, A. J.; Lee, J. Y. *Polym. Rev.* **2007**, *47*, 217–229.
(4) Jakubinek, M. B.; White, M. A.; Mu, M. F.; Winey, K. I. *Appl. Phys. Lett.* **2010**, *96*, 083105.
(5) Lee, K. S.; Smith, T. J.; Dickey, K. C.; Yoo, J. E.; Stevenson, K. J.; Loo, Y. L. *Adv. Funct. Mater.* **2006**, *16*, 2409–2414.
(6) Rowe, B. W.; Freeman, B. D.; Paul, D. R. *Polymer* **2009**, *50*, 5565–5575.
(7) Gindy, M. E.; Prud'homme, R. K. *Expert Opin. Drug Delivery* **2009**, *6*, 865–878.
(8) Keddie, J. L.; Jones, R. A. L.; Cory, R. A. *Europhys. Lett.* **1994**, *27*, 59–64.
(9) Keddie, J. L.; Jones, R. A. L.; Cory, R. A. *Faraday Discuss.* **1994**, 219–230.
(10) Fukao, K.; Miyamoto, Y. *Phys. Rev. E* **2000**, *61*, 1743–1754.
(11) Priestley, R. D.; Broadbelt, L. J.; Torkelson, J. M.; Fukao, K. *Phys. Rev. E* **2007**, *75*, 061806.
(12) Ellison, C. J.; Torkelson, J. M. *Nature Mater.* **2003**, *2*, 695–700.
(13) Yang, Z. H.; Fujii, Y.; Lee, F. K.; Lam, C. H.; Tsui, O. K. C. *Science* **2010**, *328*, 1676–1679.
(14) Peter, S.; Meyer, H.; Baschnagel, J. *J. Polym. Sci., Part B: Polym. Phys.* **2006**, *44*, 2951–2967.
(15) Rittigstein, P.; Priestley, R. D.; Broadbelt, L. J.; Torkelson, J. M. *Nature Mater.* **2007**, *6*, 278–282.
(16) Forrest, J. A.; Dalnoki-Veress, K.; Stevens, J. R.; Dutcher, J. R. *Phys. Rev. Lett.* **1996**, *77*, 2002–2005.

(17) Mattsson, J.; Forrest, J. A.; Borjesson, L. *Phys. Rev. E* **2000**, *62*, 5187–5200.
(18) Ash, B. J.; Siegel, R. W.; Schadler, L. S. *J. Polym. Sci., Part B: Polym. Phys.* **2004**, *42*, 4371–4383.
(19) Kropka, J. M.; Pryamitsyn, V.; Ganesan, V. *Phys. Rev. Lett.* **2008**, *101*, 075702.
(20) O'Connell, P. A.; McKenna, G. B. *Eur. Phys. J. E* **2006**, *20*, 143–150.
(21) Priestley, R. D.; Ellison, C. J.; Broadbelt, L. J.; Torkelson, J. M. *Science* **2005**, *309*, 456–459.
(22) Jackson, C. L.; Mckenna, G. B. *J. Non-Cryst. Solids* **1991**, *131*, 221–224.
(23) Arndt, M.; Stannarius, R.; Groothues, H.; Hempel, E.; Kremer, F. *Phys. Rev. Lett.* **1997**, *79*, 2077–2080.
(24) Huwe, A.; Kremer, F.; Behrens, P.; Schwieger, W. *Phys. Rev. Lett.* **1999**, *82*, 2338–2341.
(25) Kremer, F.; Huwe, A.; Arndt, M.; Behrens, P.; Schwieger, W. *J. Phys.: Condens. Matter* **1999**, *11*, A175–A188.
(26) Fukao, K.; Miyamoto, Y. *Phys. Rev. E* **2001**, *6401*, 011803.
(27) Roth, C. B.; Dutcher, J. R. *Eur. Phys. J. E* **2003**, *12*, S103–S107.
(28) Sasaki, T.; Shimizu, A.; Mourey, T. H.; Thurau, C. T.; Ediger, M. D. *J. Chem. Phys.* **2003**, *119*, 8730–8735.
(29) Park, C. H.; Kim, J. H.; Ree, M.; Sohn, B. H.; Jung, J. C.; Zin, W. C. *Polymer* **2004**, *45*, 4507–4513.
(30) Raegen, A.; Massa, M.; Forrest, J.; Dalnoki-Veress, K. *Eur. Phys. J. E* **2008**, *27*, 375–377.
(31) Priestley, R. D.; Mundra, M. K.; Barnett, N. J.; Broadbelt, L. J.; Torkelson, J. M. *Aust. J. Chem.* **2007**, *60*, 765–771.
(32) Sharp, J. S.; Forrest, J. A. *Phys. Rev. Lett.* **2003**, *91*, 235701.
(33) Papaleo, R. M.; Leal, R.; Carreira, W. H.; Barbosa, L. G.; Bello, I.; Bulla, A. *Phys. Rev. B* **2006**, *74*, 094203.
(34) Qi, D.; Fakhraai, Z.; Forrest, J. A. *Phys. Rev. Lett.* **2008**, *101*, 096101.
(35) Priestley, R. D. Effects of Nanoscale Confinement and Interfaces on the Structural Relaxation of Amorphous Polymers Monitored at the Molecular Scale by Fluorescence and Dielectric Spectroscopy. Northwestern University, Evanston, IL, 2008.
(36) McKenna, G. B. *Eur. Phys. J. Spec. Top.* **2010**, *189*, 285–302.
(37) Forrest, J. A.; Dalnoki-Veress, K.; Dutcher, J. R. *Phys. Rev. E* **1997**, *56*, 5705–5716.
(38) Fakhraai, Z.; Forrest, J. A. *Phys. Rev. Lett.* **2005**, *95*, 025701.
(39) Efremov, M. Y.; Olson, E. A.; Zhang, M.; Zhang, Z.; Allen, L. H. *Phys. Rev. Lett.* **2003**, *91*, 085703.
(40) Efremov, M. Y.; Olson, E. A.; Zhang, M.; Zhang, Z. S.; Allen, L. H. *Macromolecules* **2004**, *37*, 4607–4616.
(41) Lu, H. Y.; Chen, W.; Russell, T. P. *Macromolecules* **2009**, *42*, 9111–9117.
(42) Erber, M.; Tress, M.; Mapesa, E. U.; Serghei, A.; Eichhorn, K. J.; Voit, B.; Kremer, F. *Macromolecules* **2010**, *43*, 7729–7733.
(43) Still, T.; Sainidou, R.; Retsch, M.; Jonas, U.; Spahn, P.; Hellmann, G. P.; Fytas, G. *Nano Lett.* **2008**, *8*, 3194–3199.
(44) Rharbi, Y. *Phys. Rev. E* **2008**, *77*, 031806.
(45) Robertson, C. G.; Hogan, T. E.; Rackaitis, M.; Puskas, J. E.; Wang, X. *J. Chem. Phys.* **2010**, *132*, 104904.
(46) Schonhals, A.; Stauga, R. *J. Chem. Phys.* **1998**, *108*, 5130–5136.
(47) Schonhals, A.; Goering, H.; Schick, C. *J. Non-Cryst. Solids* **2002**, *305*, 140–149.
(48) Schonhals, A.; Goering, H.; Schick, C.; Frick, B.; Zorn, R. *Eur. Phys. J. E* **2003**, *12*, 173–178.
(49) Schonhals, A.; Goering, H.; Schick, C.; Frick, B.; Zorn, R. *Colloid Polym. Sci.* **2004**, *282*, 882–891.
(50) Schonhals, A.; Goering, H.; Schick, C.; Frick, B.; Zorn, R. *J. Non-Cryst. Solids* **2005**, *351*, 2668–2677.
(51) Anastasiadis, S. H.; Karatasos, K.; Vlachos, G.; Manias, E.; Giannelis, E. P. *Phys. Rev. Lett.* **2000**, *84*, 915–918.
(52) Elmahdy, M. M.; Chrissopoulou, K.; Afratis, A.; Floudas, G.; Anastasiadis, S. H. *Macromolecules* **2006**, *39*, 5170–5173.
(53) Chrissopoulou, K.; Anastasiadis, S. H.; Giannelis, E. P.; Frick, B. *J. Chem. Phys.* **2007**, *127*, 144910.
(54) Fotiadou, S.; Chrissopoulou, K.; Frick, B.; Anastasiadis, S. H. *J. Polym. Sci., Part B: Polym. Phys.* **2010**, *48*, 1658–1667.
(55) Zhang, L.; D'Acunzi, M.; Kappl, M.; Auernhammer, G. K.; Vollmer, D.; van Kats, C. M.; van Blaaderen, A. *Langmuir* **2009**, *25*, 2711–2717.
(56) Forrest, J. A.; Mattsson, J. *Phys. Rev. E* **2000**, *61*, R53–R56.
(57) Torres, J. A.; Nealey, P. F.; de Pablo, J. J. *Phys. Rev. Lett.* **2000**, *85*, 3221–3224.
(58) Long, D.; Lequeux, F. *Eur. Phys. J. E* **2001**, *4*, 371–387.
(59) Baljon, A. R. C.; Billen, J.; Khare, R. *Phys. Rev. Lett.* **2004**, *93*, 255701.
(60) Herminghaus, S.; Seemann, R.; Landfester, K. *Phys. Rev. Lett.* **2004**, *93*, 017801.
(61) Seemann, R.; Jacobs, K.; Landfester, K.; Herminghaus, S. *J. Polym. Sci., Part B: Polym. Phys.* **2006**, *44*, 2968–2979.
(62) Meng, Y.; Simon, S. L. *J. Polym. Sci., Part B: Polym. Phys.* **2007**, *45*, 3375–3385.
(63) Gaur, U.; Wunderlich, B. *Macromolecules* **1980**, *13*, 1618–1625.